Structural optimization of ring resonant cavity consisted with symmetry prisms

Yao Chengkang, Li Jun, Li Long

(AVIC Xi′an Flight Automatic Control Research Institute, Xi′an 710075, China)

Abstract: The amplitude of the output voltage signal of ring resonator which consisted of right trapezoid prisms would be modulated in the mechanical vibration. From the perspective of engineering exploration, a new symmetry structure compacted with symmetry prisms to improve the ring resonator performance was put forward and discussed in the first time. The propagation property of the laser beam and the stress distribution in prisms of those two kinds of resonators was analyzed by theoretical computation and finite element analysis method. Results show that, as for the laser resonator that wavelength is 632.8 nm, the symmetry structure has a symmetry stress distribution, and the value is much lower than that in asymmetry one in prism by 15%. Compared with the asymmetry cavity′s output energy, the deviation extent of the symmetry one decreased more than 52.63% in one excitation period. From the results of simulation, using the symmetry resonator structure could reduce the stress induced birefringence in prism and off-axis range of the laser beam trajectory in the cavity, and improve the stability of output laser intensity and output signal quality effectively. The symmetry structure provides a new way for optimization design and reduction amplitude modulation for the ring resonator.

Key words: ring resonant cavity; light intensity modulation; stress induced birefringence

CLC number: TN252; V241.558 **Document code:** A **DOI:** 10.3788/IRLA201645.1118002

对称棱镜式环形谐振腔结构优化

姚呈康,李 俊,李 龙

(中航工业西安飞行自动控制研究所,陕西 西安 710075)

摘 要: 由直角梯形棱镜构成的环形谐振腔的输出信号在机械振动环境下会受到影响,使输出波形幅值产生调制。为了改善谐振腔输出信号质量,从工程探索的角度出发,首次将对称型全反射棱镜纳入谐振腔的结构设计方案中。通过理论计算和有限元分析的方法,对比了两种谐振腔的光线传输特性和应力分布。结果表明,对于传输波长为 632.8 nm 的激光谐振腔而言,对称型结构可以保证构成谐振腔的光学元件具有对称的应力分布,降低棱镜上的应力双折射效应,提高输出信号的稳定性。对称性棱镜环形谐振腔的激光传输轨迹更稳定,装配要求更宽松,应力极值仅为非对称结构的 15%。通过对比,在一个激励周期内,对称型谐振腔的激光输出能量波动相比原始结构降低了 52.63%,平稳性获得

收稿日期:2016-03-15; **修订日期:**2016-04-23

作者简介:姚呈康(1985-),男,高级工程师,博士,主要从事谐振式光纤陀螺方面的研究。Email:yaochengkang@126.com

了显著的改善。使用对称型环形谐振腔,对于提高我国现阶段环形激光传感器件的输出稳定性提供了一种新的技术途径。

关键词:环形谐振腔; 光强调制; 应力双折射

0 Introduction

Ring resonant cavity appeared to be a key part of laser inertia measurement device for this instant influence on measurement precision[1-3]. At present, there are just two kinds of laser resonant cavity types which are consisted with right trapezoid prisms and that with coating reflector. The prisms cavity, which processes many advantages such as wide applied field, stable performance and high abilities of preventing interference, has drawn much attention in recent years. In engineering practical use, it is found that the amplitude of the output light signal of a prism laser cavity is always modulated by mechanical dither of basement, which decreases the output quality of resonant laser[4-5]. Xie Yuanping explained the mechanism of that mechanical dither which could modulate the output′s light intensity based on self-consistent theory for ring laser resonator[6]. Wan el al. indicate that the mechanical dither of biasing system brings alternating force to the optical devices in laser resonator and thus makes the cavity length varied, which decreased the frequency stabilities of output light [7]. These papers mostly explained the phenomena that the resonator cavity′s output performance degeneration in the mechanical environment in principle. Nevertheless, researches about the structure optimization for output light′s intensity of prism ring resonant cavity rarely saw to be reported yet.

In this paper, the propagation property in resonant cavity and the stress distribution in right trapezoid prisms were analyzed. Based on those results, a new structure scheme that using symmetry prisms to accomplish the ring resonant cavity was introduced firstly. By means of coinciding the center symmetry axis of four symmetry prisms and ring resonator cavity, the cavity and prisms realized fewer stress value and symmetry stress distributions. The laser propagation trajectory, optical stability, assembling tolerance and prism stress distribution property of those two kinds of cavities was compared and analyzed by using light transfer matrix and finite element method. The symmetry structure scheme presented in this paper would provide an important reference for optimizing the structure design and improving the reliability of prism laser resonator cavity.

1 Theoretical model

The output light intensity stability of the quadrangle resonant cavity, which consisted of right trapezoid prisms, could become worse due to the defect of asymmetric structure under mechanical dither situation. In this paper, the ABCD matrix method was adopted to calculate the prism assembling error influence for certain resonant cavity.

Figure 1 shows the half section view of resonant cavity and laser propagating diagram for asymmetry structure, which consisted of four right trapezoid

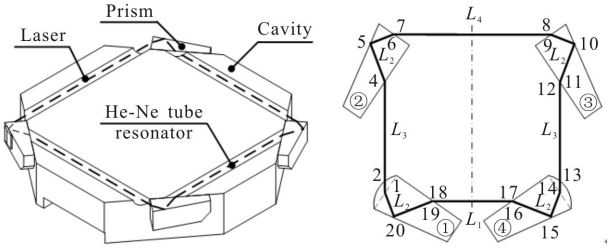

(a) Half section view of resonant cavity (b) Laser propagating diagram

Fig.1 Laser transmission diagram in trapezoid prisms resonant cavity

prisms of refractive index 1.457 38, He-Ne gas [8], which sealed in the columniform tunnel resonator by vacuum process using prisms, produces a laser beam

of wavelength 632.8 nm.

In Fig.1 (b), 1−20 represent the position of light transmission in different medium surface, and $L1-L4$ represent the light transmission length in the same medium. On the basis of laser transmission theory, this paper uses position parameters (r, a) of paraxial ray to analyze the light trajectory, where r is the length from the paraxial ray to optical axis in medium surface, a is the angle from that. Table 1 listed the light transfer and perturbation matrices for light trapezoid prisms. Where

Tab.1 Light transfer and perturbation matrices for right trapezoid prisms

	From air to prism	From prism to air
Transfer matrix	$\begin{bmatrix} n & 0 \\ -\frac{(n^2-1)\sqrt{n^2+1}}{n^2R} & \frac{1}{n^2} \end{bmatrix}$	$\begin{bmatrix} \frac{1}{n} & 0 \\ -\frac{(n^2-1)\sqrt{n^2+1}}{nR} & n^2 \end{bmatrix}$
Δn perturbation matrix	$\begin{bmatrix} \frac{1}{n} & 0 & 0 \\ -\frac{(n^2-1)\sqrt{n^2+1}}{nR} & n^2 & -\Delta n_Q+n\Delta n_A \\ 0 & 0 & 1 \end{bmatrix}$	$\begin{bmatrix} n & 0 & 0 \\ -\frac{(n^2-1)\sqrt{n^2+1}}{nR} & \frac{1}{n^2} & -\frac{\Delta n_Q}{n^2}+\frac{\Delta n_A}{n^2} \\ 0 & 0 & 1 \end{bmatrix}$
$\Delta\alpha$ perturbation matrix	$\begin{bmatrix} n & 0 & 0 \\ -\frac{(n^2-1)\sqrt{n^2+1}}{(1+n\Delta\alpha)n^2R} & \frac{1}{n^2} & \left(1-\frac{1}{n^2}\right)\Delta\alpha \\ 0 & 0 & 1 \end{bmatrix}$	$\begin{bmatrix} \frac{1}{n} & 0 & 0 \\ -\frac{(n^2-1)\sqrt{n^2+1}}{(n+\Delta\alpha)R} & n^2 & (n^2-1)\Delta\alpha \\ 0 & 0 & 1 \end{bmatrix}$

n is the refractive index of the prism, R is the curvature radius of the surface between the prism and air. Δn_Q, Δn_A are the refractive index change for prism and air respectively. $\Delta\alpha$ is angle perturbation value for prism manufacture. In accordance with the above matrices from Tab.1, the variation of laser intensity under mechanical dither could be derived. Light offset for resonant cavity could be computed by light transfer matrix, which is obtained by multiplying the transfer matrix at every medium surface inversely from an arbitrary point of the annular optical trajectory to the start point. Moreover, the influence caused by environmental change and manufacture error mainly affect meridian light. Table 1 just listed meridian transfer matrix, while the matrix for sagittal light could be obtained as presented way. When analyzing the optical stability condition, both meridian and sagittal light should be calculated as the same method.

During the dither period, the practical optic axis always departs ideal position due to the prism stress, temperature effect and manufacturing error of prisms. This variation is time-dependent such as that of stress. Research has shown that tress and temperature induced refractive index change in the key factor of periodically change for the output light intensity of the resonant cavity [9]. The stress-induced index ellipsoid equation of prism and linear stress question set is listed as follows:

$$\begin{cases} \sum (B_{ij}^{0}+\Delta B_{ij})x_i x_j=1 & i,j=1,2,3 \\ \Delta B_{ij}=\prod_{ijkl}\sigma_{kl} & i,j,k,l=1,2,3 \end{cases} \tag{1}$$

Where ΔB_{ij} is the refractive index change of the prism under the periodical stress, x_1, x_2, x_3 are three dimensional coordinates of the prism. σ_{kl} represents stress. $\prod_{ijkl}$ is the piezo-optical of efficiency of prism material[10].

As for the ring resonant cavity concerned, the influence of temperature works not only in prisms, but also in sealed air. The range of temperature for cavity′s working environment is from minus 40 ℃ to 60 ℃. In such large variation range, the larger size of prism, the stronger the thermally induced refractive index change effect. The material of the prism this paper discussed is fused silica, and the relationship

between refractive index and temperature is expressed as follows:

$$n_p=n_{p0}+K(\lambda)T \tag{2}$$

Where n_{p0} is the refractive index of the prism in room temperature (25 ℃). T is absolute temperature. $K(\lambda)$ is the temperature coefficient at a particular light wavelength of material.

As for the air index model, which was defined by experimental determination, was established by measuring the air temperature of the laboratory every hour for one week, and using linear fitting method to deal with the experimental data. The experimental relationship between air index and temperature is listed as follows:

$$n_a(T)=1+\frac{n_{a0}-1}{1+\alpha T} \tag{3}$$

Where n_{a0} is the refractive index of air in 0 ℃, which is around 1.000 32. α is the constant coefficient 0.003 68 $℃^{-1}$. In the range of 100 ℃ temperature variations, that of air index is around 0.000 086.

When calculating the optical axis deviation for the resonant cavity, the perturbation optical axis could be considered as the paraxial ray of ideal optical axis based on the light transfer theory. Assuming the coordinates of the initial light′s position is (r_0,a_0), while (r,a) for the positon after one cycle transfer, the entire loop transfer matrix T for laser resonator could be obtained by multiplicating the perturbation matrix inversely. If (r,a) equals to (r_0,a_0), the new optical axis satisfies the self consistency condition. According to self consistent principle, the (r_0,a_0) which satisfy the above condition could be calculated as follows:

$$\begin{cases} r_0=\dfrac{(1-a_{22})a_{13}+a_{12}a_{23}}{2-a_{11}-a_{22}} \\ a_0=\dfrac{(1-a_{11})a_{23}+a_{21}a_{13}}{2-a_{11}-a_{22}} \end{cases} \tag{4}$$

Where a_{ij} $(i,j=1,2,3)$ in Eq.(4) is the matrix element of T at row i and column j.

The direct influence of axis deviation is changing the optical length and the area enclosed by the ring light path. As for the light path shown in Fig.1(b), the optical length of ring resonator could be obtained as follows:

$$d_{常温}=4(h_1+h_2)n_{p0}+\frac{4(R-\sqrt{R^2-(z/2)^2})}{z\times\sin\theta_B}(z-y)n_{p0}+ L_1n_{HN}+2L_3+L_4n_{a0} \tag{5}$$

Where h_1, h_2 are the optical length in prism respectively. z is the length of shorter side of right trapezoid prism. y is the distance between exit point in one prism and incidence point in another one. θ_B is the brewster angle. L_1, L_3, L_4 are distance that light transmission presented in Fig.1(b). n_{HN} is the refractive index of He-Ne gas.

When temperature changes, the refractive index and cavity deformation are changing at the same time. The optical length of that moment is determined as follows:

$$d_T=\left[4(h_1+h_2)+2\frac{(R-\sqrt{R^2-(z/2)^2})}{\frac{z}{2}\sin\theta_B}(z-y)\right]n_T(1+\alpha_1T)+ (L_1n_{HN}+2L_3+L_4n_{0T})(1+\alpha_2T) \tag{6}$$

Where α_1 and α_2 are the coefficient of thermal expansion for quartz prism and cavity material, n_{0T} is the refractive index of air under the temperature of T, while n_T is that of prisms.

All the influential factors presented above could have an obvious effect on intensity signal of output light. The mode parameters for resonator cavity of laser, which has a fundamental Gaussian mode [11], could be varied according to the different prism structure parameters and manufacture situation in stable dither condition. As a result, this paper treated the laser intensity variation as the output signal for the resonator cavity. Let photodetector surface be XOY plane, the maximum energy point as the origin, the direction of light propagating as z axis, then the electrical field intensity of light E, which described with the spatial coordinate(x,y,z), could be depicted as follows:

$$E(x,y,z)=\frac{a_0}{\omega(z)}\times\exp\left[-\frac{x^2+y^2}{\omega^2(z)}\right]\times \exp\left[-ik\left(\frac{x^2+y^2}{2R(z)}+z\right)+\mathrm{i}\varphi(z)\right] \tag{7}$$

Where a_0 is the amplitude of the electrical field, $\omega(z)$

is the radius of the Gaussian light spot at z, $R(z)$ is the curvature radius of the phase plane in z for the Gaussian light.

According to Eq. (7), the distribution of light intensity of ring resonator cavity is calculated as follows:

$$I(x,y)=I_0\exp\left[\frac{-2(x^2+y^2)}{\omega_0^2}\right]=I_0\exp\left[\frac{-2r^2}{\omega_0^2}\right]=I(r) \tag{8}$$

As for the situation that adopting diaphragm to suppress the high order mode, the power of laser without optical axis deviation is calculated as follows:

$$P_0=\int_S I(r)2\pi r\mathrm{d}r=\frac{\pi\omega_0^2 I_0}{2}\left[1-\exp\left(-\frac{2Da^2}{\omega_0^2}\right)\right] \tag{9}$$

Where r is the distance between given point and spot center, S is the area of diaphragm, Da is the apertures diameter. When light deviated from axis, the practical light power through the diaphragm is depicted as follows:

$$P_d=\begin{cases}-\dfrac{\omega_0^2 I_0}{4}\displaystyle\int_0^{2\pi}\left\{\exp\left[-\frac{2}{\omega_0^2}R_+^2(\theta)\right]-1\right\}\mathrm{d}\theta, & 0<d<Da\\ -\dfrac{\omega_0^2 I_0}{4}\displaystyle\int_{-\arcsin(Da/d)}^{\arcsin(Da/d)}\left\{\exp\left[-\frac{2}{\omega_0^2}R_+^2(\theta)\right]-\exp\left[-\frac{2}{\omega_0^2}R_-^2(\theta)\right]\right\}\mathrm{d}\theta, & Da<d\end{cases} \tag{10}$$

Where,

$$\begin{cases}R_+^2(\theta)=(d\cos\theta+\sqrt{d^2\cos^2\theta-d^2+Da^2})\\ R_-^2(\theta)=(d\cos\theta-\sqrt{d^2\cos^2\theta-d^2+Da^2})\end{cases} \tag{11}$$

2 New resonator structure design

The existing prism for ring resonator cavity is right trapezoid structure. For the quadrilateral closed loop resonator, there are three requirements that the prism must meet. First of all, the incidence angle from air to prism should be equal to that from prism to air, which is the Brewster angle of the prism. Secondly, the intersection angle between the incident ray and exit should be equal to 90°. At last, the reflection angle in prism should be greater than the critical angle of total reflection of prism. Taking all above requirements into consideration, Fig.2(a) shows a new prism structure, while Fig.2(b) shows a quadrilateral resonator consisted of these prisms.

Figure 2 shows a better symmetry than original structure presented in Fig.1. There are two symmetry axes in the new resonator. Furthermore, the light propagating trajectory is closer to circular. If the number of prisms increases, the ratio between area and perimeter of light trajectory is greater than that of original one′s.

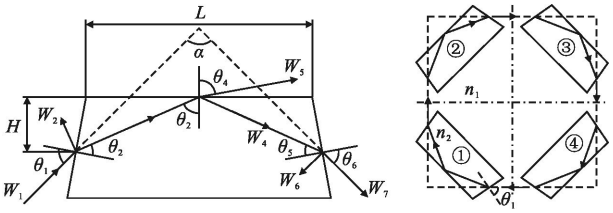

(a) Light propagating though a symmetrical prism (b) Symmetrical ring resonator cavity

Fig.2 Schematic diagram of symmetrical ring resonator structure

As for the light trajectory shown in Fig.2(a), the energy of light could be calculated based on the Fresnel equation as follows:

$$\begin{cases}W_{3p}=\dfrac{\sin2\theta_1\sin2\theta_2}{\sin^2(\theta_1+\theta_2)\cos^2(\theta_1-\theta_2)}\\ W_{3s}=\dfrac{\sin2\theta_1\sin2\theta_2}{\sin^2(\theta_1+\theta_2)}\end{cases} \tag{12}$$

In order to compare the performance of two kinds of resonator cavity, this paper adopted certain resonator cavity size based on the principles that both structures have the same ratio between area and perimeter, the same mass, and the same optical length in each prism. The simplified model this paper analyzed is adopted as Fig.3 shows, and some complicated structures such as He-Ne tube resonator are omitted in the figure.

As shown in Fig.3, the optical length for Fig.3(a) is 258.122 4 mm, area of light trajectory is 3 379.793 mm^2,

ratio of area and perimeter is 13.094. While that of Fig.3 (b) are 228.858 4 mm, 2 998.055 mm^2 and 13.100. For both ring resonant cavity, the equivalent optical length is 67.622 4 mm.

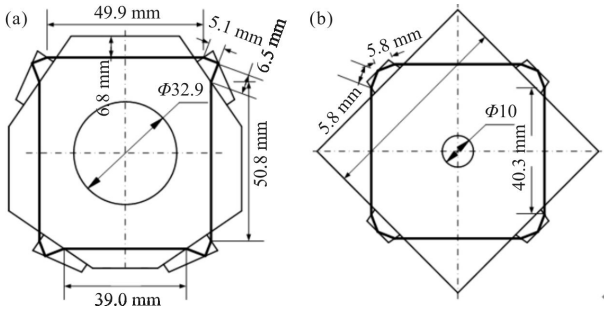

(a) Asymmetrical ring resonator cavity (b) Symmetrical ring resonator cavity

Fig.3 Simplified models for the two prism ring resonator cavity

3 Experiment and discussion

3.1 Analysis of optical stability

According to the light transfer matrix listed in Tab.1, the analysis of optical stability for the simplified model shown in Fig.3 could be calculated. The analysis parameters are listed in Tab.2.

Tab.2 Analysis parameters of optical stability for tow kinds of resonator cavities

Resonator	Optical length/ mm	L_1/mm	L_2/mm	L_3/mm	L_4/mm	Refractive index
Asymmetry	258.12	39.0	11.6	50.8	49.9	1.457 38
Symmetry	228.86	40.3	11.6	40.3	40.3	1.457 38

Let the position 1, which is shown in Fig.1(b), as the start point of light trajectory. Calculating the transfer matrix T_G by travelling around the resonator cavity in a clockwise direction. Define F_{os} as the factor of optical stability which could be calculated as:

$$F_{os}=\left|\frac{1}{2}(T_{G11}+T_{G22})\right|<1 \tag{13}$$

The relationship between curvature radius R of prism surface and and F_{os} listed in Eq.(13) for the two kinds of resonators are depicted in Fig.4.

Figure 4 shows the difference between the two structures based on the simplified model, which is listed in Tab.3.

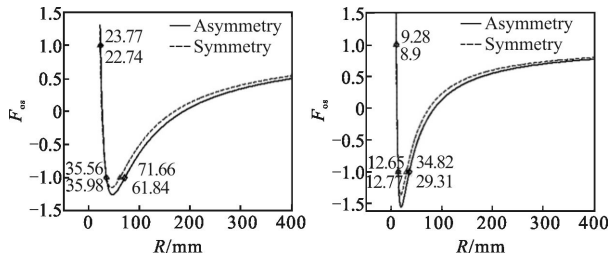

(a) Meridian surface (b) Sagittal surface

Fig.4 Factor of optical stability for each resonator cavity

Tab.3 Difference between the two structures

Resonator	Meridian/mm	Sagittal/mm	Curvature radius/mm
Asymmetry	23.77<R<35.56 71.66<R	9.28<R<12.65 34.82<R	R>71.66
Symmetry	22.74<R<35.98 61.84<R	23.77<R<35.56 71.66<R	R>61.84

According to the results listed in Tab.3, the requirement of curvature radius of symmetry is more relaxed than that of asymmetry, which is demanded to be above 61.84 mm.

3.2 Analysis of axis deviation

When the light wavelength is 632.8 nm, taking surface machining error and temperature induced refractive index change into consideration, the analyzing results are presented in Fig.5 about deviation situations of distance and angle at each position shown in Fig.1 (b) at −100 ℃, −50 ℃, 0 ℃, 50 ℃, 100 ℃, under dither condition for resonator cavity based on Eq.(2)−Eq.(4) with the help of light transfer matrix listed in Tab.1.

Figure 5 shows the symmetry results of new structural cavity for error and perturbation. Within specified range of temperature change, the axis deviation of symmetry cavity is smaller than that of asymmetry one′s [12]. Based on these results, the change in light intensity of the resonator cavity could be obtained using Eq. (9) −Eq. (10). As for the simplified model, assuming that in the original laser, P light and S light have an equivalent amount and the

refractive index of prisms is 1.457 38, the output energy of two kinds of cavities under 400 Hz dither drive is listed in Tab.4.

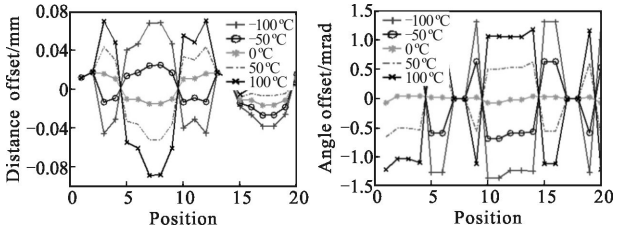

(a) Distance offset for symmetry (b) Angle offset for symmetry

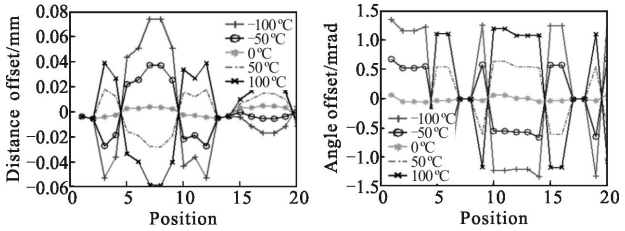

(c) Distance offset for asymmetry (d) Angle offset for asymmetry

Fig.5 Ptical axis offset for two resonator under different temperature and surface machining error

Tab.4 Energy statistics for two kinds of resonator under dithered environment

Resonator	Energy means	Energy standard deviation	Variation range
Asymmetry	70.238%	6.815×10^{-3}	2.09%
Symmetry	228.86 mm	3.226×10^{-3}	0.98%

From Tab.4, it is presented that energy deviation ranges of the ring resonator cavity consisted of symmetry prisms is reduced to 52.63%, which shows an obvious advantage in laser energy stability.

3.3 FEA for two structures

For the simplified models Fig.3 presented, the stress distribution and dynamic response for the two kinds of cavity structures were discussed by finite element analysis (FEA) method. The analysis parameters are listed in Tab.5.

Tab.5 FEA parameters for two structures

	Elasticity modulus /GPa	Flexural strength /GPa	Thermal expansivity /℃$^{-1}$	Poisson coefficient	Density /kgm^{-3}
Cavity	92	0.14	9×10^{-3}	0.28	2 457
Prism	72	0.06	115×10^{-3}	0.17	2 200

According to the practical use, the element nodes were loaded a sinusoidal excitation signal in the first order resonant frequency of each structure. The stress distribution results of prisms were calculated in 50 substeps during one excitation period. Figure 6 shows typical analysis results in 5 substeps among that for two kinds of prisms. The five figure listed above from *a*1 to *a*5 in Fig.6 showed the asymmetry prism′s stress distribution, while the five figures below presented the symmetry one′s.

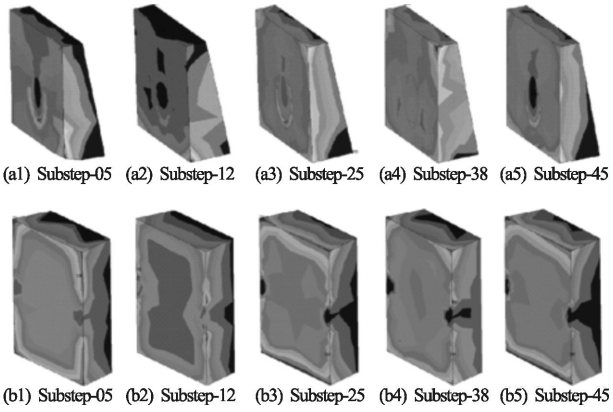

Fig.6 Stress distribution results for two prisms in 5 analysis substeps

This simulation results demonstrated that symmetry prisms have much smaller stress amount than that of asymmetry prism, and the stress distributions are symmetrical also. The specific statistic at the above 5 substeps Fig.6 adopted is listed in Tab.6.

Tab.6 Extremum results for two prisms at different substeps

Substep		Asymmetry	Symmetry	Ratio value
5	SMN	0.003 701	0.007 459	201.54%
	SMN	0.445 865	0.436 248	97.84%
12	SMN	0.181 643	0.028 054	15.44%
	SMN	6.189 000	0.981 899	15.87%
25	SMN	0.526 938	0.036 345	6.90%
	SMN	12.235 000	1.657 000	13.54%
38	SMN	0.147 638	0.017 473	11.84%
	SMN	7.454 000	0.828 948	11.12%
45	SMN	0.339 224	0.031 877	9.40%
	SMN	15.786 000	1.503 000	9.52%

It is obvious from the results listed in Tab.6 that at the same substep, the stress value of symmetry prism is always much smaller than that of asymmetry, which remains 15% of asymmetry prisms have. Based on the results above, using symmetry prism in ring resonator cavity could reduce stress induced influence in dither drive, which is helpful to improve the laser transfer stability effectively.

In order to compare the performance of two prisms in stress distribution, stress deviations in a prism of 3 nodes that light trajectory travelling across the medium surface was analyzed during one dither period. The nodes selecting ways were presented as Fig.7.

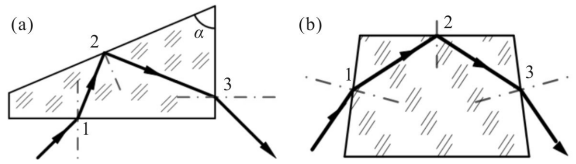

Fig.7 Nodes selecting ways of two prisms

The stress distribution curve of the 3 nodes Fig.7 shows for two prisms was depicted in Fig.8 and Fig.9.

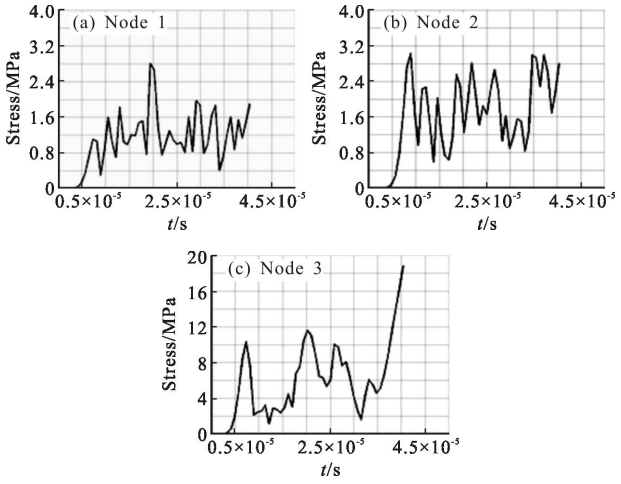

Fig.8 Stress-time curve for asymmetry prism in one excitation period

Based on the analysing results Fig.9 showed, not only the stress value but also the distribution is not similar between these two prism structures. The stress value of asymmetry is always greater than that of symmetry prism, and its distribution does not have any regularity. While the symmetry prism, by contrast, has good similarity between nodes 1 and node 3. All the results demonstrated that the stress distribution performance of symmetry prism is much better than that of asymmetry prism.

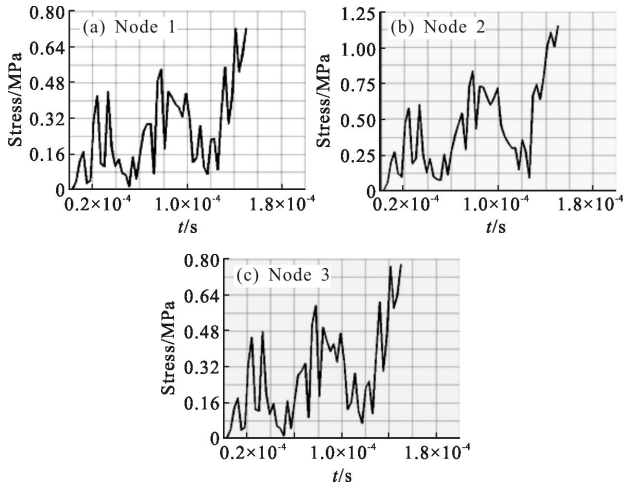

Fig.9 Stress-time curve for symmetry prism in one excitation period

4 Results

In this paper, a new ring resonator cavity consisted of symmetry prisms has been presented and discussed firstly from the perspective of engineering exploration. As for the practical using, the amplitude of the output voltage signal of the existing resonator cavity, which is consisted of right trapezoid prisms, always appears to be modulated in the mechanical vibration. To contrast the performance of output light of different cavities such as optical stability, axis offset, stress distribution, light transfer matrix and FEA method were adopted to analyse the difference. According to the analysis results, the new symmetry cavity has obvious inhibition ability for the circumstance influence, of which the deviations are symmetrical also. By comparing the output energy, deviation extent the symmetry cavity′s result was down more than 52.63% from that of asymmetry one′s in one excitation period, which could improve the output stability effectively. These analyse results discussed in this paper, would provide an important reference for optimizing the structure design and improving the reliability of resonator cavity.

References:

[1] Duan Xuechao, Qiu Yuanying, Duan Qingjuan, et al. Calibration and motion control of a cable driven parallel manipulator based triple level spatial positioned [J]. ***Advances in Mechanical Engineering***, 2014, 6(2): 306018.

[2] Yao Chengkang, Li Qinghui. Motion compensation realization for satellite borne camera [J]. ***Infrared and Laser Engineering***, 2011, 40(6): 1090-1097.

[3] Wang Zhiguo, Long Xingwu, Wang Fei, et al. Bias characteristics of a multioscillator ring laser gyro with consideration of differential losses [J]. ***Optics & Laser Technology***, 2013, 48(7): 285-293.

[4] Jiang Qiyuan, Tang Jianxun, Yuan Baolun, et al. Analysis and compensation for size effect error of laser gyro strapdown inertial navigation system [J]. ***Infrared and Laser Engineering***, 2015, 44(4): 1110-1114. (in Chinese)

[5] Gao Bolong, Zhang Mei, Zhang Wen. New interpretation of laser gyro drifts [J]. ***Science China Technological Sciences***, 2010, 53(5): 1168-1175.

[6] Yuan Baolun, Han Songlai, Yang Jianqiang, et al. Rotation scheme for single-axis indexing RLG INS [J]. ***Journal of Chinese Inertial Technology***, 2011, 19(2): 145-151.

[7] Jiang Shaodong, Su Yan, Shi Qin, et al. Theory and experimental modal analysis of dual-mass vibrating silicon micro-gyroscope [J]. ***Optics and Precision Engineering***, 2015, 23(2): 467-476. (in Chinese)

[8] Liu Yaoying, Xue Chenyang, Zheng Hua, et al. Structure design and optimization of high fineness ring resonator [J]. ***Infrared and Laser Engineering***, 2014, 43(11): 3688-3693. (in Chinese)

[9] Schereiber K U, Gebauer A, Velikoseltsev A, et al. Precision cavity control for the stable operation of a large ring laser gyroscope [C]//IEEE, Laser Optics International Conference, 2014: 14545119.

[10] Guo Ning, Qin Fuxiang, Meng Qingyou, et al. Analysis on stress birefringence of panda polarization-maintaining optical fiber with external force [J]. ***Optics & Optoelectronic Technology***, 2008, 6(5): 38-41. (in Chinese)

[11] Shi Zhen, Chen Shuai, Zhang Jian, et al. Temperature compensation of laser gyro based on improved RBF neural network [J]. ***Optics and Precision Engineering***, 2014, 22 (11): 2975-2982. (in Chinese)

[12] Xu Guangming, Wang Fei. Ring laser gyro light path variations and its impact on gyro performance [J]. ***Journal of Applied Optics***, 2010, 31(5): 805-809.